to excrete NO_3^- in the urine for at least 20 days. The total excess urinary NO_3^- was 1 to 2.5 g. However, the assumption of a nitrification process in the gut cannot be interpreted properly unless values for the total body content of NO_3^- and NO_2^- are known. We have been unable to find such values in the literature. Radomski *et al.* (*1*) have also commented on the lack of available information about the body disposition of NO_3^-. They point out the difficulties associated with assaying NO_3^- and in excluding this ion from food and drinking water. However, a rough estimate of 1 g for the total body content of NO_3^- can be made from the data in Table 1 if the following assumptions are made: (i) intravenous $^{13}NO_3^-$ equilibrates with body NO_3^- in 40 minutes; (ii) the bladder contained 250 ml of urine; and (iii) the concentration of NO_3^- in urine was 100 mg/liter reported by Radomski *et al.* (*1*). Since this is the same order of magnitude as the excess urinary excretion reported by Tannenbaum *et al.* (*12*) and since $^{13}NO_3^-$ was distributed very evenly, it seems possible that their results could be explained (at least in part) as due to the slow washout of NO_3^- from the body. Furthermore, the ^{13}N data in rats may help explain the intestinal values of NO_3^- and NO_2^- reported by Tannenbaum *et al* (*12*). Although a major percentage of the ^{13}N appears to be absorbed from the upper intestinal tract, clearly it is not entirely removed as suggested by Hill and Hawksworth (*13*). Therefore, direct passage of NO_3^- and NO_2^- down the gut, which previously was though not to occur, in conjunction with the secretion of bloodstream (or biliary and pancreatic) NO_3^- into the intestinal lumen (which an intestinal alteration, that is, colectomy, may enhance) could account for the presence of NO_3^- and NO_2^- in the ileostomy and fecal samples as reported (*12*).

Further work should be done to delineate whether these intestinal and urinary concentrations of NO_3^- and NO_2^- are the result of dietary intake, slow release of body stores, or bacterial nitrification in the intestinal tract (*12*). Since the last of these explanations would represent an unavoidable exposure to these ions and hence the possibility for a "complete" endogenous formation of carcinogenic *N*-nitroso compounds, its importance is obvious.

JAMES P. WITTER
S. JOHN GATLEY
EDWARD BALISH
Departments of Medical Microbiology, Radiology, and *Surgery, University of Wisconsin Medical School, Madison 53706*

References and Notes

1. J. L. Radomski, C. Palmiri, W. L. Hearn, *Toxicol. Appl. Pharmacol.* **45**, 63 (1978).
2. F. Joliot and I. Curie, *Nature (London)* **133**, 201 (1934).
3. M. G. Straatman, *Int. J. Appl. Radiat. Isot.* **28**, 13 (1977).
4. R. Gersberg, K. Krohn, N. Peek, C. R. Goldman, *Science* **192**, 1229 (1976).
5. J. S. Laughlin, R. S. Benva, R. S. Tilbury, Progress Report CHOO-4268-1 to the Energy Research and Development Administration, Washington, D.C. (September 1977); K. A. Krohn and N. J. Parks, *J. Labelled Compd. Radiopharm.* **16**, 87 (1979).
6. An Anger camera consists of a single crystal of NaI (doped with thallium) typically 1 cm thick and 30 cm in diameter. A lead collimator in front of the crystal improves resolution at the expense of sensitivity. Signals from 20 or more photomultipliers behind the crystal are processed to give x and y coordinates of each γ-ray that produces a scintillation in the crystal. The computer synthesizes a 64 by 64 matrix picture (a "frame") from these coordinates, and the spatial resolution is about 1 cm. Nuclear medicine imaging and other procedures are described in *A Textbook of Nuclear Medicine Technology*, P. J. Early, M. A. Razzak, B. Sodee, Eds. (Mosby, St. Louis, 1975).
7. The results in Table 1 can be approximately related to one another because the total counts were measured in an internal organ (the stomach) where conditions for the attenuation of radiation would be similar to those for salivary glands and the bladder. Furthermore, the attenuation of 0.511-MeV radiation by tissue is not great.
8. S. R. Tannenbaum, M. C. Archer, J. S. Wishnok, W. W. Bishop, *J. Natl. Cancer Inst.* **60**, 251 (1978).
9. C. F. Wang, R. G. Cassens, W. G. Hoekstra, unpublished information summarized in a symposium held in 1973 at the Food Research Institute of the College of Agriculture and Life Sciences of the University of Wisconsin-Madison.
10. H. S. Grindley and W. J. MacNeal, in "Studies in nutrition; An investigation of the influence of saltpeter on the nutrition and health of man with reference to its occurrence in cured meats" (Univ. of Illinois, Champaign, 1917), vol. 1, chap. 1, pp. 9-36.
11. In similar intravenous studies with humans using $^{13}NH_4^+$, we found that the salivary glands do not "concentrate" ^{13}N as they do when $^{13}NO_3^-$ is injected.
12. S. R. Tannenbaum, D. Fett, V. R. Young, P. D. Land. W. R. Bruce, *Science* **200**, 1487 (1978).
13. M. J. Hill and G. M. Hawksworth, in *N-Nitroso Compounds: Analysis and Formation*, P. Bogovski, R. Pressmann, E. A. Walker, Eds. (International Agency for Research on Cancer, Lyon, France, 1972), p. 116.
14. S.J.G. thanks the Wellcome Trust for a travel grant. We thank the University of Wisconsin physics staff for generous allocation of accelerator time [Energy Research and Development Administration grant EY-76-C-02-0007-00 (Task A), NCI 5PO1CA 19278-03]; Dr. R. J. Nickels for supplying us with $^{13}NO_3^-$; G. D. Peterson, C. Kan, B. Johnson, and J. Brown for help with the animal experiments; and D. Brackett for her patience in manuscript preparation.

13 November 1978; revised 12 January 1979

Influence of Cartilage Geometry on the Pressure Distribution in the Human Hip Joint

Abstract. *To elucidate the role of mechanical factors in the etiology of osteoarthritis, the detailed geometry of the weight-bearing cartilage layer over the human hip socket is compared with the corresponding pressure distribution. The shape of the pressure distribution is strongly correlated with the shape of the cartilage compression distribution.*

Articular cartilage is a remarkable bearing material that can provide a lifetime of trouble-free movement of synovial joints. Often, however, signs of cartilage deterioration are seen in the joints of middle-aged persons, and the incidence and severity of degeneration generally increase with age (*1*). Despite many nutritional, biological, and biochemical studies (*2*), the cause of osteoarthritis is still unknown. More recently, researchers have emphasized the importance of understanding the frictional, wear, and mechanical behavior of articular cartilage—that is, lubrication mechanisms, anisotropic, poroelastic, and viscoelastic properties, and fatigue strength (*3*). To understand the mechanical environment in which articular cartilage must exist in vivo, we developed a new, more accurate description of the global shape and thickness of acetabular cartilage by using ultrasonics and compared this geometry with the corresponding surface pressure distribution on loaded acetabula from cadavers.

The pressure distribution is of particular importance for understanding the par-

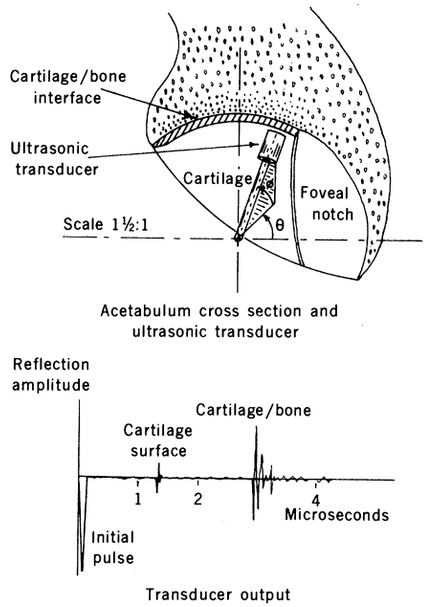

Fig. 1. Schematic representation of the ultrasonic transducer scanning technique used to measure hip joint geometry.

0036-8075/79/0427-0413$00.50/0

titioning of load between the solid cartilage matrix and the synovial fluid, and therefore the tribology and state of stress on and in articular cartilage. Other researchers indirectly assessed the surface pressure at a few spatially separate sites and inferred an axisymmetric sinusoidal pressure distribution (*4*). We developed an instrumented endoprosthesis for direct measurement of the spatial and temporal pressure distribution over the human acetabulum (*5*) and found nonaxisymmetric irregular pressure distributions (*6*). To explain these unusual distributions, we sought to quantify the cartilage geometry.

The shape of the human hip joint has been studied for more than 100 years by use of calipers, three-legged micrometers, projected radiographs, circular templates, and dial-gauge profilometers (*7*), but these techniques tend to average the radius of curvature over a fairly large area of arc and can easily miss local deviations from sphericity. It is also difficult to transform these measurements into three-dimensional descriptions. Excluding radiographs, the measuring devices in these techniques touch, and possibly distort, the cartilage surface. Localized cartilage thickness measurements have been made by invasive techniques (*8*). We developed a noninvasive, noncontact method that improves local accuracy and produces global data, including the cartilage thickness distribution.

An ultrasonic transducer rotating in spherical coordinates scans the cartilage surface (Fig. 1). Reflection times from the transducer to the cartilage surface and to the calcified interface covering the subchondral bone and back, together with local sound-propagation velocities, give the distances from the transducer to the cartilage surface and to the calcified interface. Computer programs are used to determine the spheres that best fit the cartilage surface and calcified interface data and produce contour plots that indicate elevations and depressions relative to the spherical surfaces (*9*).

Acetabula obtained at autopsy are submerged in saline solution at body temperature and aligned in the hip simulator so that the resultant force vector replicates the direction in vivo. First, the unloaded acetabular cartilage geometry is measured by the ultrasonic technique. Then, using the spherical pseudofemoral head with internal pressure instrumentation, forces in the physiological range are applied and the pressure distributions are recorded. The position of the ball in the socket under load is determined by using a sphere identical to the pressure-instrumented unit but with a flush-mounted ultrasonic transducer. Rotation of this sphere about its geometric center, for the same load and time after loading as the pressure-instrumented unit, yields localized position information relative to the calcified interface. By geometric reconstruction, the thickness distribution of the cartilage under load can be calculated.

The data presented are typical of results for six normal specimens (*10*). Acetabular geometry data are shown in Fig. 2. The outer kidney-shaped solid line is the perimeter of the cartilage layer covering the acetabulum. Figure 2, A and B, shows the deviations from sphericity of the cartilage surface and calcified interface, respectively. The cartilage surface is spherical, with localized maximum deviations less than 150 μm. The calcified interface has much larger deviations, up to 500 μm, which show the ability of cartilage to compensate for an irregular bony foundation. We found that the lateral region of the cartilage is generally thicker than the medial region (Fig. 2C). The center of the best-fitting sphere through the cartilage surface is positioned 300 μm medially and 400 μm anteriorly relative to the center of the sphere representing the calcified interface; the magnitude of this medial shift tends to be larger for older specimens.

Figure 3A is the pressure distribution contour map of the same specimen when loaded at 2.5 times body weight, within the physiological range. Since cartilage is poroelastic, consolidation occurs. The data shown were taken 30 seconds after the application of a step force along the load direction in vivo. A universal joint in the loader allows the ball to assume natural alignment with the socket. No other relative motion between ball and

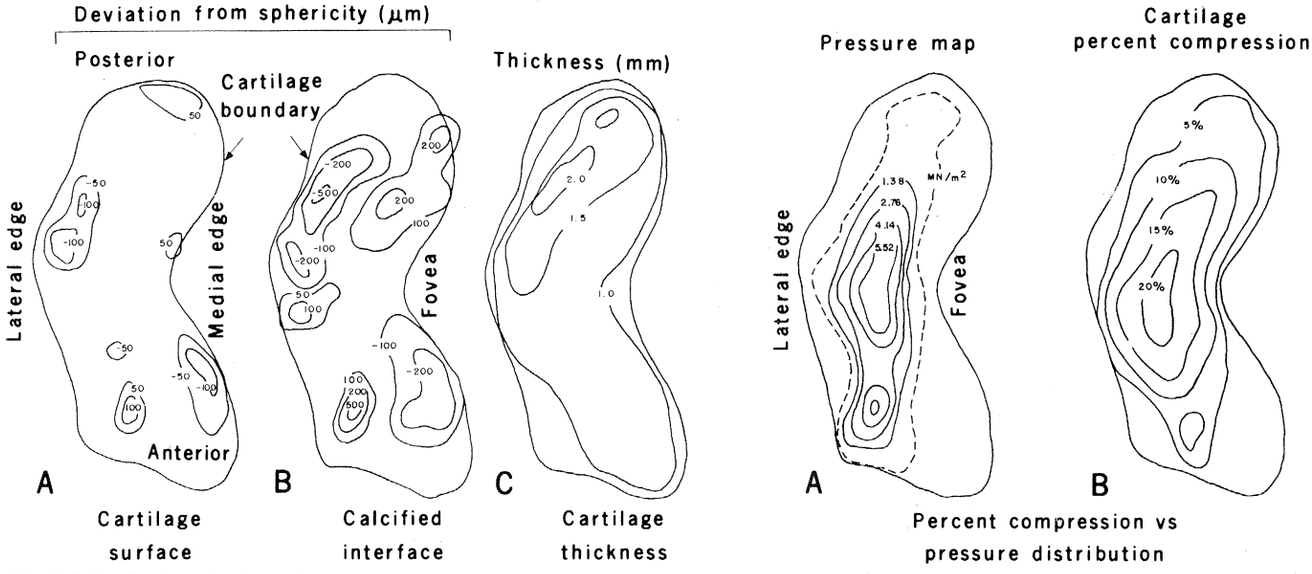

Fig. 2 (left). Conic projections about the resultant force vector looking into the zenith of the acetabulum, showing (A) cartilage surface deviation from sphericity, (B) calcified interface deviation from sphericity, and (C) acetabular cartilage thickness. Approximately 150 spatially independent points separated by 10° latitude and 10° longitude were measured and the best-fitting sphere was found by least-squares for the cartilage surface and calcified interface. The negative sign denotes valleys. Fig. 3 (right). (A) Pressure distribution for a 1350-N load applied to the acetabulum. The dashed line is the edge of the contact area. The contour plot was interpolated from 253 data points. Maximum pressure was 6.8 MN/m² and average pressure was 2.5 MN/m². (B) Percentage compression of the cartilage layer calculated from the geometry data and the position of the ball in the socket.

socket was imposed. The elongation of the pressure distribution in the anterior to posterior direction and the multiple local maxima are typical.

Comparison of the shape of the contours of percentage cartilage compression (Fig. 3B) with the surface pressure distribution (Fig. 3A) shows a strong correlation between the acetabulum geometry and the surface stress on articular cartilage. These data suggest that abnormal hip joint geometry, either congenital or due to trauma, will cause stress concentrations in the cartilage layer. Since abnormal hip joint geometry is often observed in osteoarthritis (*11*), the correlation between geometry and stress contributes to the understanding of the etiology of osteoarthritis.

PAUL D. RUSHFELD*
ROBERT W. MANN
WILLIAM H. HARRIS†
Department of Mechanical Engineering, Massachusetts Institute of Technology, Cambridge 02139

References and Notes

1. M. A. R. Freeman, *Adult Articular Cartilage* (Grune & Stratton, New York, 1972); P. D. Byers, C. A. Contepomi, T. A. Farkas, *Ann. Rheum. Dis.* **29**, 15 (1970).
2. A. J. Bollet, J. L. Nance, *J. Clin. Invest.* **45**, 1170 (1966); M. Brookes and B. Helal, *J. Bone Jt. Surg. Br. Vol.* **50**, 184 (1968); H. J. Mankin and L. Lippiello, *J. Bone Jt. Surg. Am. Vol.* **52**, 424 (1970); A. Maroudas, T. Bullough, S. A. V. Swanson, M. A. R. Freeman, *J. Bone Jt. Surg. Br. Vol.* **50**, 166 (1968).
3. D. Dowson, *Proc. Inst. Mech. Eng.* **182**, 68 (1968); W. C. Hayes and L. F. Mockros, *J. Appl. Physiol.* **31**, 562 (1971); G. R. Higginson, M. R. Litchfield, J. Snaith, *Int. J. Mech. Sci.* **18**, 481 (1976); B. Weightman, *J. Biomech.* **9**, 193 (1976).
4. A. S. Greenwald and J. J. O'Connor, *J. Bone Jt. Surg. Br. Vol.* **54**, 157 (1972); W. H. Day, S. A. V. Swanson, M. A. R. Freeman, *ibid.* **57**, 302 (1975); G. Piotrowski, thesis, Case Western Reserve University (1975).
5. C. E. Carlson, R. W. Mann, and W. H. Harris, [*IEEE Trans. Biomed. Eng.* **BME-21**, 257 (1974)] describe the in vivo version of the pressure-instrumented pseudofemoral head used in the in vitro experiments described here. The pressure transducers consist of 14 diaphragms machined into the inside of the load-bearing hemisphere. Each diaphragm is 3 mm in diameter and 0.25 mm thick. Pressure on the diaphragm produces center deflection, which is transmitted to a small cantilever made of silicon with a strain gauge bridge diffused onto its surface. Bending of the beam causes a change in output voltage proportional to the magnitude of the applied pressure in the range 0 to 11 MN/m². The prosthesis is mounted in an electrohydraulic hip joint simulator (*6*), which can replicate the loads and motions of the human hip joint. Rotation relative to the acetabulum of the endoprosthesis sphere about its geometric center sweeps the pressure transducers across the load-bearing surface. Pressure signals from the 14 transducers are time-multiplexed and transmitted to a Digital PDP 11/40 computer, where an interpolation routine produces and plots the pressure contours.
6. P. D. Rushfeldt, D. W. Palmer, R. W. Mann, W. H. Harris, in *Proceedings: AAMI 13th Annual Meeting 1978* (Association for the Advancement of Medical Instrumentation, Arlington, Va., 1978), p. 225.
7. B. T. Hammond and J. Charnley, *Med. Biol. Eng.* **5**, 445 (1967); P. Bullough, J. Goodfellow, A. S. Greenwald, J. J. O'Connor, *Nature (London)* **217**, 1290 (1968); I. C. Clarke and H. C. Amstutz, in *The Hip* (Mosby, St. Louis, 1975), p. 63; C. G. Armstrong, thesis, Queen's University, Belfast (1977).
8. L. Sokoloff, *Fed. Proc. Fed. Am. Soc. Exp. Biol.* **25**, 1089 (1966).
9. P. D. Rushfeldt, R. W. Mann, W. H. Harris, in preparation; P. D. Rushfeldt, thesis, Massachusetts Institute of Technology (1978).
10. The specimen used for the data presented here is from the left side of a 49-year-old male weighing 52.8 kg and 168 cm tall. The acetabular diameter was equal to that of the instrumented prosthesis. Except for one calcified point on the anterior lateral region of the acetabulum, the cartilage was in generally good condition. This particular specimen was taken directly from the autopsy room to the hip simulator. Other specimens are stored in the frozen state. Experiments with the same tissue, first fresh and then after freezing, showed no change.
11. S. D. Stulberg, L. D. Cordell, W. H. Harris, P. L. Ramsey, G. D. MacEwen, in *The Hip* (Mosby, St. Louis, 1975), p. 212.
12. Supported by the Whitaker Professorship of Biomedical Engineering, Massachusetts Institute of Technology, and by NIH grant AM16116.
* Present address: Perry Oceanographics, Inc., Riviera Beach, Fla. 33404.
† Major affiliation: Hip and Implant Unit, Massachusetts General Hospital, Boston 02114.

18 September 1978; revised 11 January 1979

Natural Polyesters: Dufour's Gland Macrocyclic Lactones Form Brood Cell Laminesters in *Colletes* Bees

Abstract. *Bees in the genus* Colletes *make their brood cells in the ground and coat them with a highly resistant, waterproof, transparent membrane. This membrane is a polyester constructed mainly from 18-hydroxyoctadecanoic acid and 20-hydroxyeicosanoic acid, which are stored as their corresponding lactones in the Dufour's gland of the bee. When lining the cells, the bee secretes its glandular content, and the membrane is apparently a product of polycondensation reaction of its contents. This appears to be the first report of a naturally occurring linear polyester. The term laminester (lamina ≃ layer + ester) for this class of compounds is proposed.*

Many of the approximately 20,000 species of solitary and social bees (Apoidea; Hymenoptera) make their nests and brood cells in moist soil. The hygroscopic provision of nectar and pollen is protected against water, fungi, and various soil organisms by a layer of waterproof secretion applied by the nesting female to the soil surrounding the cell (Fig. 1). The chemical composition and origin of this secretion in most bees is unknown (*1*).

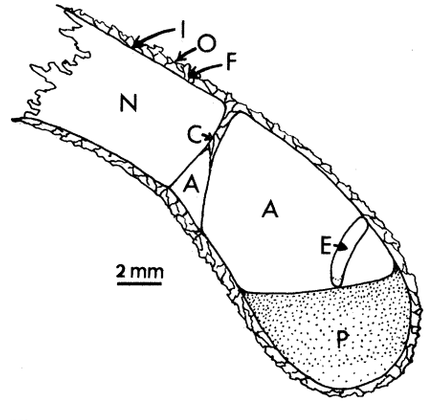

Fig. 1. Brood cell of *Colletes validus*. This semidiagrammatic drawing emphasizes the double-layered structure of this polyester membrane sac. *I*, inner layer of thick membrane; *O*, outer layer of thin, fragile membrane that adheres loosely to surrounding soil; *F*, fibrils that connect the two layers; *A*, air space found in cell cap, in cell, and between layers; *C*, double-layered membranous cell cap; *N*, neck of cell, normally filled with soil after oviposition; *E*, egg adhering to cell by cephalic end; and *P*, provision, consisting of a semiliquid mixture of pollen and nectar. Cells are made in the soil at the ends of tunnels.

As early as 1835, the Dufour's gland of *Colletes* was suspected to be the source of the cell lining (*2*), and the possible role of this gland in cell construction by other bees was also considered (*1*, *3*). These conclusions were mostly drawn on the basis of solubility tests (*1*, *3*), and of morphological (*4*) and behavioral (*5*) evidence. Recent investigations of the fragrant, oily secretion that fills the Dufour's gland in several species of bees have revealed macrocyclic lactones in *Colletes cunicularis* (*6*) and in five genera of halictine bees (*6*, *7*), and farnesyl and geranyl esters in *Andrena* spp. (*8*).

We report here chemical evidence that the cell linings of *Colletes thoracicus*, *C. inaequalis*, and *C. validus* are the polymerized secretions of the hypertrophied Dufour's glands of these bees. In order to find out if the cell lining originates from the glandular content, it was necessary to compare the chemical nature of the Dufour's gland secretion and the cell lining.

Dufour's glands dissected from the living bees were extracted with methylene chloride and analyzed by combined gas chromatography and mass spectroscopy (GC-MS) (*9*). The glands contain a mixture of macrocyclic ω-lactones, hydrocarbons, and aldehydes (Fig. 2A). The two dominant lactones are 18-octadecanolide and 20-eicosanolide, accompanied by 18-octadecenolide (of undetermined double-bond location), 22-docosanolide, a methyl-branched eicosano-

0036-8075/79/0427-0415$00.50/0